Regulation of angiogenesis and choroidal neovascularization by members of microRNA-23~27~24 clusters

Qinbo Zhou[a], Rachel Gallagher[a], Rafael Ufret-Vincenty[a], Xinyu Li[a], Eric N. Olson[b,1], and Shusheng Wang[a,c,1]

Departments of [a]Ophthalmology, [b]Molecular Biology, and [c]Pharmacology, University of Texas Southwestern Medical Center, Dallas, TX 75390

MicroRNAs (miRNAs) modulate complex physiological and pathological processes by repressing expression of multiple components of cellular regulatory networks. Here we demonstrate that miRNAs encoded by the miR-23~27~24 gene clusters are enriched in endothelial cells and highly vascularized tissues. Inhibition of miR-23 and miR-27 function by locked nucleic acid-modified anti-miRNAs represses angiogenesis in vitro and postnatal retinal vascular development in vivo. Moreover, miR-23 and miR-27 are required for pathological angiogenesis in a laser-induced choroidal neovascularization mouse model. MiR-23 and miR-27 enhance angiogenesis by promoting angiogenic signaling through targeting Sprouty2 and Sema6A proteins, which exert antiangiogenic activity. Manipulating miR-23/27 levels may have important therapeutic implications in neovascular age-related macular degeneration and other vascular disorders.

blindness | MAP kinase signaling | semaphorins | Akt | proangiogenic

The growth of blood vessels through angiogenesis is a delicately controlled process that involves endothelial cell (EC) activation, proliferation, migration, and maturation (1). Physiological angiogenesis is required for normal vascular development as well as vascular homeostasis during adulthood. Pathological angiogenesis, commonly induced by tissue ischemia or inflammation, underlies numerous vascular disorders, such as age-related macular degeneration (AMD), a leading cause of blindness in the elderly (2). Choroidal neovascularization (CNV), which involves abnormal growth of blood vessels in the back of the eye, is a hallmark of neovascular AMD (3). Although the pathogenic mechanisms underlying AMD are still largely unknown, vascular endothelial growth factor (VEGF) has been shown to play a causal role in the development of CNV (4). Anti-VEGF agents have demonstrated efficacy in treating CNV in neovascular AMD (5, 6) but have limited efficacy and potential side effects (7, 8).

Recent studies have revealed important roles for microRNAs (miRNAs) in cardiovascular diseases and other disorders (9). miRNAs are small noncoding RNAs that negatively regulate gene expression by inducing mRNA degradation or inhibiting translation through binding to the 3′ untranslated region (3′UTR) of target mRNAs (10). Often, miRNAs modulate broad collections of mRNAs encoding multiple components of complex biological pathways. Several miRNAs have been implicated in angiogenesis (11, 12). A group of miRNAs has also been shown to be substantially decreased in a laser-induced CNV model (13).

The miR-23~27~24 clusters are highly expressed in ECs (14–17). Two miR-23~27~24 clusters exist in the vertebrate genome: an intergenic miR-23a~27a~24–2 cluster and an intronic miR-23b~27b~24–1 cluster. Members of these clusters are involved in cell cycle control, proliferation, and differentiation of various cell types (18). Here, we show that inhibition of miR-23/27 impairs angiogenesis in vitro and postnatal retinal vascular development in vivo. Moreover, silencing of miR-23/27 suppresses laser-induced CNV in mice. The proangiogenic functions of miR-23/27 correlate with the repression of Sprouty2 and Sema6A, which negatively regulate angiogenic signaling.

Results

Structure and Expression Pattern of miR-23~27~24 Cluster Members.
The mouse miR-23a~27a~24–2 cluster is intergenic on chromosome 8, and the miR-23b~27b~24–1 cluster is located in intron 4 of an alanine aminopeptidase gene on chromosome 13 (Fig. 1A). The miR-23a~27a~24–2 cluster encodes a primary miRNA (pri-miRNA) transcript composed of three miRNAs: miR-23a, miR-27a, and miR-24–2, and the miR-23b~27b~24–1 cluster encodes a pri-miRNA transcript containing miR-23b, miR-27b, and miR-24–1 (Fig. S1A). The mature miRNA sequences of miR-23a/b, miR-27a/b, and miR-24 are conserved among vertebrate species (Fig. S1B). miR-23a and miR-27a differ by only one nucleotide near their 3′ ends compared with their paralogs miR-23b and miR-27b, whereas the sequence of miR-24–1 and miR-24–2 is the same (Fig. S1C). miR-23a and miR-23b share most, if not all, predicted target genes by TargetScan and DIANA Lab, as do miR-27a and miR-27b (19, 20).

Northern-blot analyses revealed that miR-23a/b, miR-27a/b, and miR-24 are expressed at the highest levels in the lung and heart, which are highly vascularized tissues (Fig. 1B). Their expression is also detectable in other organs, including the eye. Real-time PCR confirmed the enrichment of the mature miRNAs of these two clusters in the lung and heart (Fig. S1D). Real-time PCR was further performed to determine the expression of miR-23~27~24 cluster members in different cell types. Our results showed that the expression of all miR-23~27~24 cluster members is enriched in ECs compared to the other cell types tested (Fig. 1C), consistent with previous reports (14–21) and a recent report that expression of the miR-23b~27b~24-1 host gene is enriched in ECs in vivo (21). Taken together, our results indicate that miR-23~27~24 cluster members are enriched in ECs and highly vascularized tissues, suggesting a potential role in EC function.

Modulation of Sprouting Angiogenesis by miR-23 and miR-27 in Vitro.
To study the EC function of miR-23~27~24 cluster members in vitro, human umbilical vein EC line (HUVECs) were transfected with locked nucleic acid (LNA)-modified anti-miRs of miR-23a/b, miR-27a/b, or a scramble control and tested for EC network formation on Matrigel. More than 90% knockdown of miR-23a/b or miR-27a/b expression was achieved by LNA-anti-miR-23a/b or anti-miR-27a/b transfection, respectively, indicating the efficiency and specificity of miRNA knockdown by LNA anti-miRs (Fig. 2A). Hereafter, miR-23a/b and miR-27a/b will be referred to as miR-23 and miR-27. Of note, there was compensatory up-regulation of miR-23 or miR-27 when miR-27 or miR-23 were knocked down. When cultured on Matrigel, ECs form a primary vascular network. Knockdown of miR-27, and to a lesser extent miR-23, impaired the formation of capillary-like structures in HUVECs cultured on Matrigel, as quantified by the reduced branching points upon miR-27 or miR-23 inhibition (Fig. 2 B and C). These results suggest that miR-27 and miR-23 are required for proper capillary tube formation in vitro.

CELL BIOLOGY
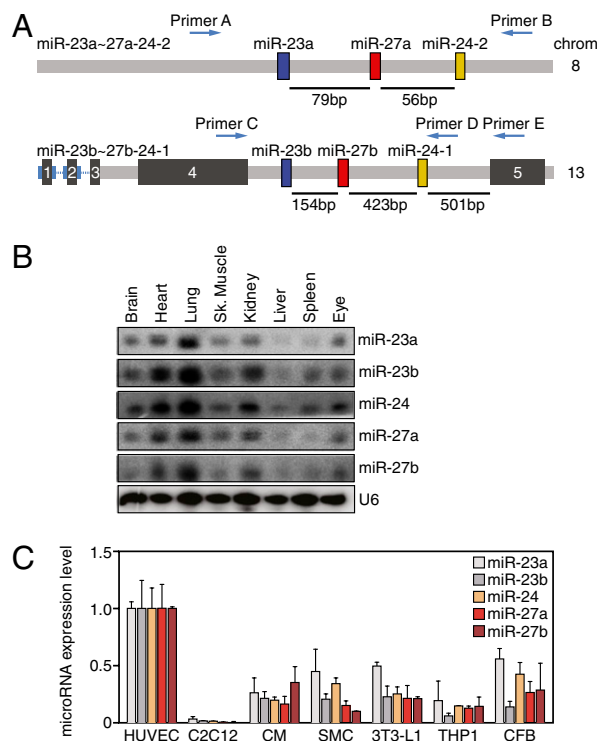
Fig. 1. Gene structure and expression pattern of miR-23~27~24 clusters. (*A*) Structure of mouse miR-23~27~24 clusters. Chromosome locations of miR-23a~27a~24–2 and miR-23b~27b~24–1 are shown. Pre-miR23a/b, pre-miR-27a/b, and pre-miR-24 are shown as colored boxes. The exons of the miR-23b~27b~24–1 host gene are indicated as black boxes. (*B*) Expression of miR-23~27~24 cluster members in different tissues as detected by Northern blot using starfire miRNA probes. U6 served as a loading control. (*C*) Expression of miR-23~27~24 cluster members in different cell types relative to that in HUVECs, as detected using LNA-modified miRNA PCR primers (Exiqon). C2C12, mouse myoblast cell line; CM, mouse cardiomyocyte; SMC, mouse smooth muscle cell line; 3T3-L1, mouse adipocyte progenitor cell line; TH1, human monocyte cell line; CFB, rat cardiac fibroblast.

Fig. 2. Regulation of angiogenesis by miR-23 and miR-27 in vitro and ex vivo. (*A*) Specific silencing of miR-23 and miR-27 in HUVECs by LNA-modified anti-miR shown by real-time PCR with LNA-modified miRNA primers. (*B*) Representative pictures of in vitro Matrigel assays after silencing of miR-23 or miR-27 in HUVECs. (*C*) Quantification of branching points in the in vitro Matrigel assays. Six independent samples were quantified in each group. *P* values are shown. (*D*) Quantification of ex vivo aortic ring assays 5 d after miR-23/27 knockdown or overexpression by adenovirus. Sprouting distance was measured from the average number of six aortic rings in each group. *P* values are indicated. ns, not significant. (*E*) Quantification of VEGF-induced HUVEC proliferation indicated by BrDU incorporation after miR-23 and/or miR-27 LNA-anti-miR transfection. *P* values are indicated. ns, not significant. (*F*) Quantification of VEGF-induced HUVEC migration distance (μm) in scratch wound assay after miR-23 or miR-27 LNA-anti-miR transfection. *P* values are indicated. ns, not significant.

An ex vivo aortic ring assay was performed to further explore the requirement of miR-23 and miR-27 in sprouting angiogenesis (22). Isolated aortic rings were transfected with anti-miR-23, anti-miR-27, or scramble control and cultured on Matrigel with endothelial growth medium supplemented with 3% mouse serum. Normally, EC sprouts appear on the second day from the aortic rings and grow rapidly after 4–6 d of culture. Compared with the control, knockdown of miR-27, and to a lesser extent miR-23, significantly repressed the outgrowth of aortic ring cells (Fig. 2*D*).

To further determine whether overexpression of miR-23 or miR-27 is sufficient to enhance sprouting angiogenesis, similar assays were performed after infection of the aortic rings with adenoviruses expressing miR-23b, miR-27b, or LacZ control. Compared with the LacZ control, overexpression of miR-27 significantly enhanced aortic ring cell outgrowth, causing an ~30% increase in migratory distance, and miR-23 overexpression also showed a trend toward increased aortic ring cell sprouting (Fig. 2*D* and Fig. S2).

To examine the cellular mechanism whereby miR-23 and miR-27 regulate angiogenesis, EC proliferation and migration were analyzed after LNA-anti-miR-23/27 transfection. EC proliferation upon VEGF stimulation was measured by BrDU incorporation, whereas EC migration was quantified after a scratch wound assay (23, 24). As shown in Fig. 2*E*, compared with serum-starved HUVECs, VEGF induced EC proliferation by ~3- fold in 24 h. Knockdown of miR-27 repressed VEGF-induced EC proliferation by ~30%, and knockdown of miR-23 also showed a trend in repressing EC proliferation. Knockdown of both miR-23 and miR-27 appeared to have a synergistic effect in repressin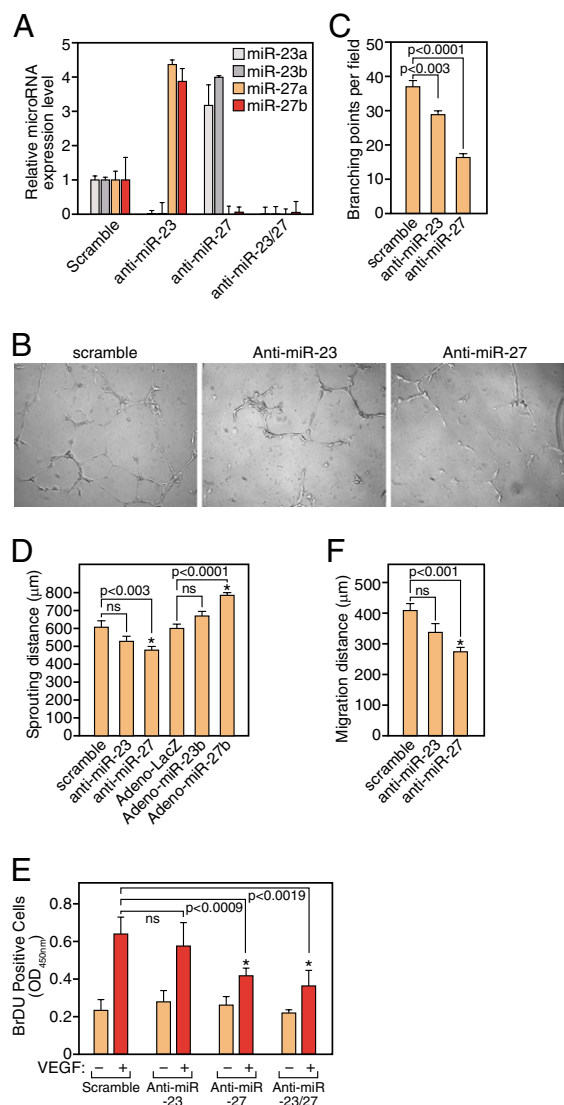g VEGF-induced EC proliferation. When a scratch wound is created in a monolayer of cultured HUVECs, the cells migrate to the wounded region upon stimulation by VEGF. VEGF-induced EC migration was significantly repressed by miR-27 silencing and to a lesser extent by miR-23 silencing in ECs (Fig. 2*F*). These results indicate that miR-23 and miR-27 enhance angiogenesis by promoting EC proliferation and migration in response to VEGF.

miR-23 and miR-27 Target Sprouty2, Sema6A, and Sema6D in ECs. To begin to elucidate the mechanisms whereby miR-23 and miR-27 regulate angiogenesis, we took a bioinformatic approach to identify signaling pathways and target genes regulated by miR-23 and

miR-27. Using the DIANA-mirPath software, designed to integrate miRNA target genes into signaling pathways (25), we found that proteins involved in axon guidance ($P = 0.00018$) and mitogen-activated protein kinase (MAPK) signaling pathways ($P = 0.034$) were significantly enriched in miR-23 and miR-27 target genes (Fig. S3A). Among the predicted target genes, we focused on Sprouty2, Semaphorin6A (Sema6A), and Semaphorin6D (Sema6D), which negatively regulate angiogenesis (26, 27). Importantly, multiple conserved binding sites for miR-23a/b and miR-27a/b are contained in the 3'UTRs of these mRNAs (Fig. S3B), suggesting that miR-23 and miR-27 might promote angiogenesis through suppression of Sprouty2, Sema6A, and Sema6D, which exert antiangiogenic activity.

To test whether miR-23 and miR-27 directly inhibit Sprouty2, Sema6A, and Sema6D 3'UTR activity, we tested the effects of these miRNAs on expression of luciferase reporters linked to the 3'UTRs of SPROUTY2, SEMA6A, and SEMA6D mRNAs in COS cells. Overexpression of miR-23 or miR-27 significantly repressed the activity of luciferase reporters containing human SPROUTY2, SEMA6A, or SEMA6D 3'UTRs (Fig. 3A). Moreover, the repression of the SPROUTY2 3'UTR by miR-23 and miR-27 was dependent on their targeting sites, because mutation of either the miR-23 target sites or the miR-27 target site in the SPROUTY2 3'UTR attenuated the repression by miR-23 or miR-27, respectively (Fig. 3A).

To examine whether miR-23 and miR-27 could repress the expression of endogenous SPROUTY2, SEMA6A, or SEMA6D proteins, HUVECs were infected with adenovirus expressing miR-23b and/or miR-27b, or LacZ as control, and SPROUTY2, SEMA6A, or SEMA6D protein expression was examined by Western blot. As shown in Fig. 3B, overexpression of miR-23b or miR-27b repressed SPROUTY2, SEMA6A, and SEMA6D proteins, whereas overexpression of miR-23b and miR-27b showed a synergistic effect in repressing the expression of these proteins. Next, we transfected HUVECs with LNA-anti-miRs of miR-23 and/or miR-27, or scramble control, and similarly examined the expression of these proteins. We observed a significant increase in the expression of SPROUTY2, SEMA6A, and SEMA6D expression upon miR-23 or miR-27 knockdown (Fig. 3B). These results indicate that miR-23 and miR-27 mediate the repression of SPROUTY2, SEMA6A, and SEMA6D expression in ECs.

Sprouty proteins function as intracellular inhibitors of the Ras/Raf/ERK pathway (28). Semaphorin proteins can provide directional cues for cell migration by modulating VEGF signaling pathways (27, 29). To test whether miR-23 and miR-27 are required for regulating angiogenic signaling pathways, HUVECs were transfected with LNA-anti-miR-23/27 or scramble control, and phospho-AKT and phospho-ERK1/2, indicative of AKT and MAPK activities, were measured. Phosphorylation of ERK1/2 and AKT was significantly decreased by miR-23 and miR-27 knockdown in ECs without affecting total ERK1/2 and AKT levels (Fig. 3C). Anti-miR-23/27 or control transfected HUVECs were further tested for ERK1/2 phosphorylation in response to VEGF. As shown in Fig. 3D, ERK1/2 phosphorylation was strongly induced in HUVECs upon VEGF treatment. Knockdown of miR-23 and miR-27 repressed ERK1/2 phosphorylation induced by VEGF, consistent with the up-regulation of the miR-23/27 target protein SPROUTY2, which inhibits the RAS/RAF/ERK pathway. SEMA6A inhibits EC migration (27). To test whether the up-regulation of SEMA6A contributes to the decreased angiogenic signaling upon miR-23/27 knockdown, HUVECs were incubated with SEMA6A recombinant protein, treated with VEGF, and tested for angiogenic signaling activities. As shown in Fig. 3E, SEMA6A significantly repressed the phosphorylation of VEGFR2 and ERK1/2 in response to VEGF, whereas VEGFR2 and ERK1/2 proteins remained unchanged. These results support the conclusion that miR-23 and miR-27 are required for modulating VEGFR2 and MAPK signaling in response to VEGF through repressing SPROUTY2 and possibly SEMA6A.

We further asked whether Sprouty2 can mediate the angiogenic effects of miR-23 and 27. Aortic ring assays were performed to examine whether knockdown of Sprouty2 by siRNA could rescue the sprouting defects caused by miR-23/27 silencing. Western blot
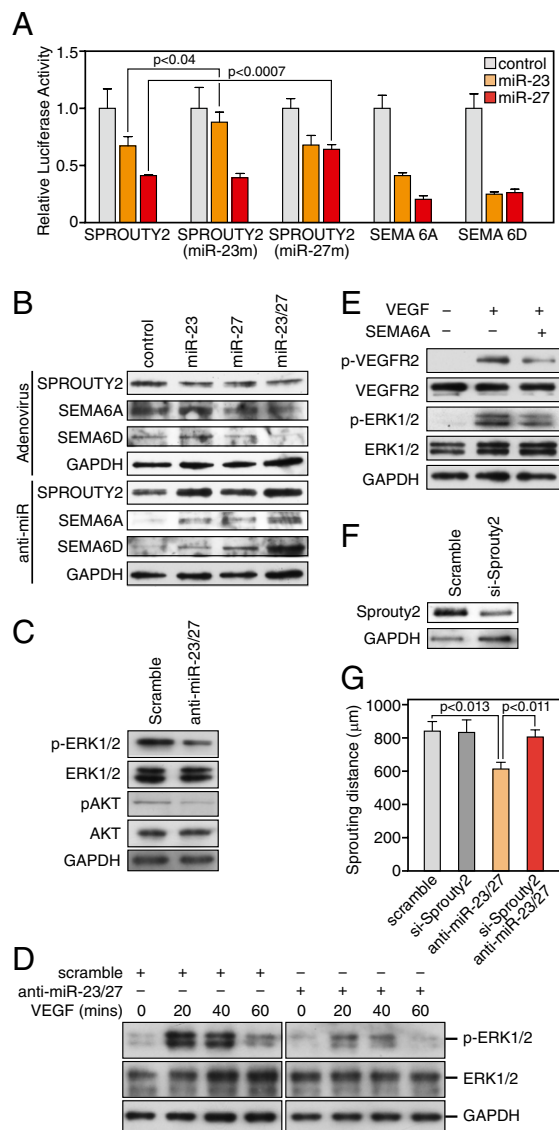

Fig. 3. Regulation of angiogenic signaling by miR-23 and miR-27. (A) miRs-23/27 target the SPROUTY2, SEMA6A, and SEMA6D 3'UTRs as shown by luciferase assays. SPROUTY2 (miR-23m) and SPROUTY2 (miR-27m) indicate SPROUTY2 UTR with mutations in miR-23 and miR-27 targeting sites, respectively. Pre-miR miRNA precursors (ABI) used in the transfections are indicated. The P values are shown. (B) Regulation of miRs-23/27 target proteins SPROUTY2, SEMA6A, and SEMA6D by miR-23 and miR-27, as detected by Western blot. LNA-anti-miR transfection or adenovirus infection was performed as indicated. (C) Repression of ERK1/2 and AKT phosphorylation by miRs-23/27 knockdown in HUVECs as shown by Western blot analyses. GAPDH served as a loading control. (D) Repression of ERK1/2 phosphorylation in response to VEGF by miRs-23/27 knockdown as shown by Western blot. LNA-anti-miR transfection and the time points of VEGF treatment are shown as indicated. (E). Repression of VEGFR2 and ERK1/2 phosphorylation in response to VEGF by recombinant SEMA6A protein as detected by Western blot. GAPDH served as a loading control. (F) Knockdown of Sprouty2 by siRNA in cultured aortas shown by Western blot. GAPDH served as a loading control. (G) Quantification of ex vivo aortic ring assays 6 d after miR-23/27 anti-miR and/or Sprouty2 siRNA transfection. Six independent aortic rings were quantified in each group. P values are indicated.

analysis confirmed the efficient Sprouty2 knockdown in the cultured aortic rings (Fig. 3F). The results showed that Sprouty2 knockdown rescued the sprouting defects caused by miR-23/27 silencing, indicating that Sprouty2 plays a major role in mediating miR-23/27 angiogenic effects (Fig. 3G and Fig. S4).

Regulation of Retinal Vascular Development by miR-23 and miR-27 in Vivo. To further address the role of miR-23 and miR-27 in angiogenesis in vivo, we performed miRNA loss-of-function studies in neonatal mouse retinas, a well-established model of angiogenesis (30). Vascularization of the outer retina commences at postnatal d 0 (P0) from the central retinal artery, and the ECs sprout to reach the peripheral region at about P8. Anti-miRs targeting miR-23 and miR-27, or scramble control, were injected intravitreously into the eye at P2, and retinas were isolated at P6 for RNA, protein, and flat mount staining of the developing retinal vasculature (Fig. 4A). Subretinal injection of LNA-anti–miR-23/27 resulted in >90% reduction in retinal miR-23/27 levels compared with the controls (Fig. 4B). Of note, compensatory up-regulation of miR-24 was observed (Fig. 4B). Thus, LNA-anti-miRs displayed high efficacy and specificity in the retina in vivo.

To examine the effect of miR-23/27 knockdown on postnatal retinal vascular development, P6 retinal flat mounts were stained with intercellular adhesion molecule-2 (ICAM-2) to visualize the vessels. Scramble LNAs did not affect retinal vascular development compared with the noninjection controls, based on ICAM-2 staining. However, in anti-miR-23/27-injected retinas, there was an ~10% decrease in sprouting distance and an ~20% decrease in vascular coverage at 4 d after anti-miR-23/27 injection compared with the controls (Fig. 4 C and D). At higher magnification, fewer newly formed vessel sprouts were observed in the anti-miR-23/27-injected retinas compared with the controls (Fig. 4C, c and d). During retinal vascular development, ECs sprout along glial fibrillary acidic protein (GFAP)-positive astrocytes. GFAP staining indicated that astrocyte coverage was not affected by miR-23/27 knockdown (Fig. 4C, e and f), suggesting that the retinal EC sprouting phenotype evoked by miR-23/27 knockdown is not secondary to potential astrocyte defects. Moreover, consistent with our in vitro results, miR-23 and miR-27 target proteins, Sprouty2, Sema6A, and Sema6D, were significantly up-regulated upon miR-23/27 knockdown in the retinas (Fig. 4E). Taken together, our results indicate that miR-23 and miR-27 modulate retinal vascular development in vivo.

Requirement of miR-23 and miR-27 in CNV in Vivo. The angiogenic defects resulting from miR-23 and miR-27 knockdown in vitro and in vivo suggested that miR-23 and miR-27 might play an important role in neovascularization in response to injury. We adopted a laser-induced CNV mouse model, the most reliable CNV animal model, to test the role of miR-23 and miR-27 in CNV (31). We first examined the expression of miR-23~27~24 clusters in the retina/choroid after laser injury. Adult C57BL/6 mice were subjected to rupture of Bruch's membrane in six locations by laser photocoagulation (140 mV, 100 ms, 100 μm) (32). As demonstrated by real-time PCR, miR-23a, miR-27a, and miR-24 levels were significantly up-regulated, and miR-23b and miR-27b expression was also increased in the retinal/choroidal region at 1 wk after laser injury (Fig. 5A).

To directly test the requirement of miR-23/27 in CNV, LNA-anti-miRs targeting miR-23 and miR-27, or scramble control, were intravitreously injected to knockdown miR-23 and miR-27 in the eye immediately following laser injury in three locations (Fig. 5B). A secondary injection was performed on the following day to ensure efficient knockdown. Eyes were collected at 2 wk after laser injury for ICAM-2 staining and confocal imaging (33). As shown in Fig. 5C, >90% knockdown efficiency of miR-23 and miR-27 in the retina/choroid/sclera was achieved by anti-miR injection compared with the controls. Of note, we observed an up-regulation of miR-23~27~24 members after scramble control injection compared with noninjection controls, possibly reflecting the increased inflammatory response due to injection. We tested anti-platelet/endothelial cell adhesion molecule (PECAM)-1 antibody, isolectin-B4, and FITC-dextran staining besides anti-ICAM-2 staining and found ICAM-2 gave the best staining for CNV, consistent with a recent report (33). Quantification of the CNV area, as shown by ICAM-2 staining, revealed that silencing of miR-23 and miR-27 repressed the CNV area by >50% compared with scramble control (Fig. 5 D and F). The repression of CNV by miR-23/27 was also confirmed by ICAM-2 staining of the lesion
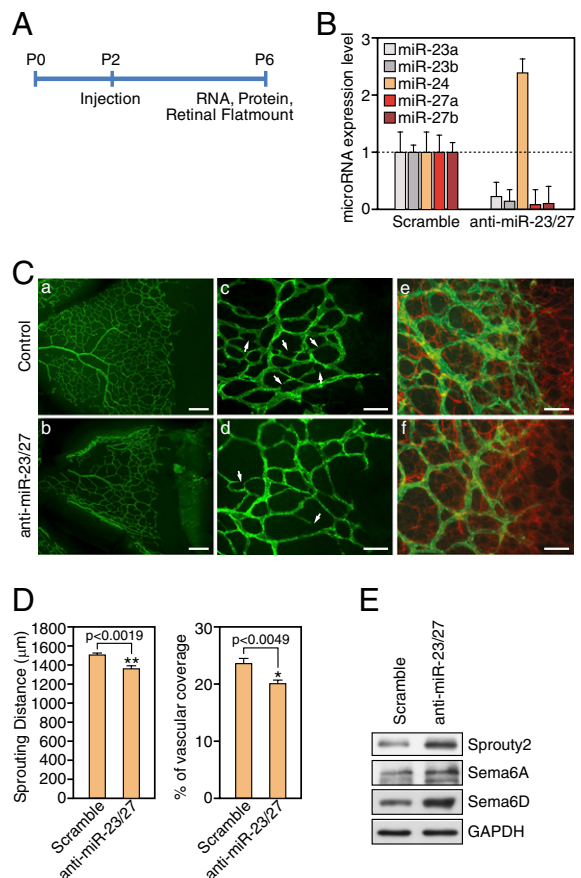

Fig. 4. Regulation of retinal vascular development by miR-23 and miR-27. (*A*) Experimental setup for retinal injections. LNA-anti-miRs were injected at P2 and retinal samples are collected at P6 for RNA, protein analyses, and flatmount staining. (*B*) Detection of miR-23~27~24 family members in the retina after LNA anti-miR treatment by real-time PCR with LNA-modified miRNA primers. (*C*) Vasculature of the retina at P6 after LNA anti-miR treatment at P2, as visualized by ICAM-2 (green) and GFAP (red) staining in flat mount preparation. Anti-scramble (*Upper*) and anti-miR-23/27 (*Lower*). Scale bar (*Left*): 100 μm. Scale bar (*Middle* and *Right*): 50 μm. Arrows point to the new retinal vascular sprouts. (*D*) Quantification of sprouting distance (μm) and vascular coverage of the retinal vasculature from 12 miR-23/27 anti-miR treated retinas compared with 12 scramble controls. *P* values are indicated. (*E*) Western blot analyses showing the up-regulation of miRs-23/27 target proteins Sprouty2, Sema6A, and Sema6D upon miRs-23/27 knockdown in P6 retinas.

sections (Fig. 5E). Compared with the noninjection controls, we observed a mild increase in CNV in scramble-injected samples, possibly due to increased CNV induced by miR~23~27~24 up-regulation (Fig. S5B). Taken together, our data indicates that miR-23 and miR-27 are required for laser-induced CNV in vivo.

Discussion

The findings of this study reveal an important role for miR-23 and miR-27 in angiogenesis and CNV (Fig. 6). We provide evidence that silencing of miR-23 and miR-27 represses sprouting angiogenesis in vitro and in vivo, as well as CNV in a laser-induced CNV mouse model. The proangiogenic actions of miR-23 and miR-27 correlate with the repression of their target mRNAs encoding Sprouty2 and Sema6A, which negatively regulate MAPK and VEGFR2 signaling in response to angiogenic factors. Thus, in the absence of miR-23 and miR-27, Sprouty2 and Sema6A proteins are up-regulated, with consequent dampening of MAPK and VEGFR2 signaling. Conversely, overexpression of miR-23 and miR-27 represses these targets, relieving their repressive influence on these pathways.
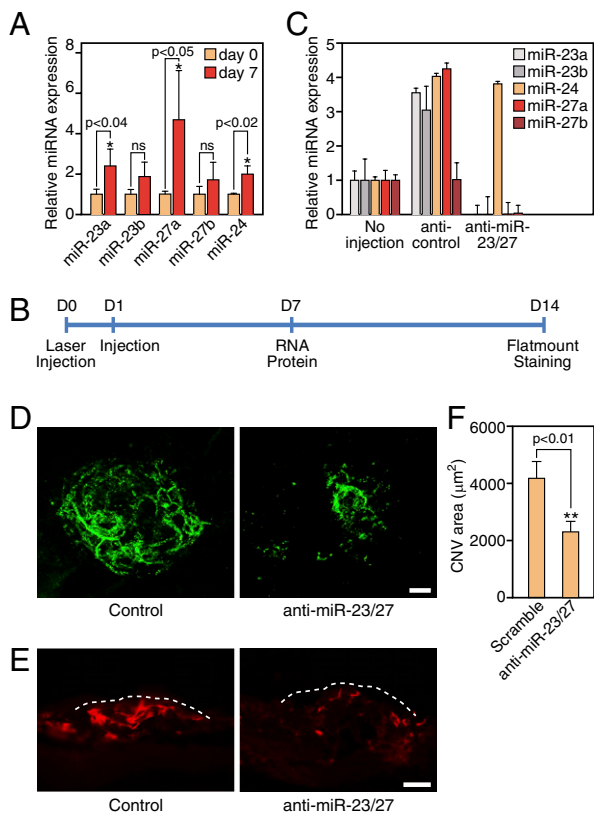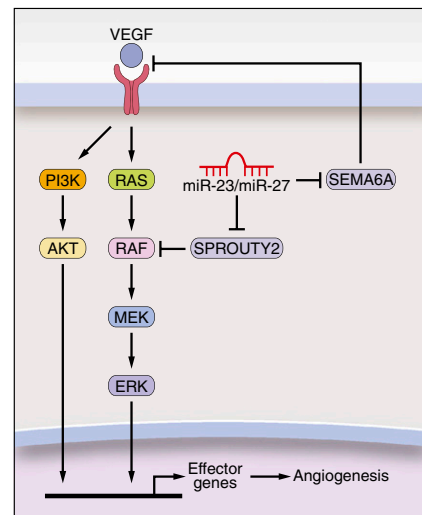
Fig. 6. A model for miRs-23/27 function in angiogenesis. VEGF binds to its receptors and activates MAP and PI3K-AKT kinase signaling pathways in ECs, which in turn stimulates the transcription of genes involved in angiogenesis. miRs-23/27 from the miR-23~27~24 families promote angiogenesis by repressing their target proteins SPROUTY2 and SEMA6A, which negatively regulate Ras/MAPK signaling and VEGFR2 mediated signaling, respectively. Loss of miR-23/27 function diminishes MAPK and VEGFR2 signaling in response to VEGF, and thereby represses angiogenesis.

Fig. 5. Repression of laser-induced CNV by LNA-anti-miR-23/27. (*A*) Up-regulation miR-23~27~24 cluster members 7 d after laser injury in the eye as shown by real-time PCR using LNA-miRNA primers. *P* values are indicated. (*B*) Experimental setup for laser injury and retinal injections. Time points of laser injury, anti-miR injection, and sample isolation are denoted below the line. (*C*) Silencing of miR-23 and miR-27 in the retina/choroid/sclera by LNA-anti-miR injection shown by real-time PCR with LNA-miRNA primers. (*D*) Representative confocal images of ICAM-2 staining showing repression of CNV by LNA-anti-miR-23/27 compared with a scramble control. Scale bar: 50 μm. (*E*) ICAM-2 immunostaining of CNV lesion sections showing reduced neovascularization by LNA-anti-miR-23/27. Dashed lines: borders the CNV lesion. Scale bar: 50 μm. (*F*) Quantification of CNV area (μm²). *P* value is from the measurements of 36 control-injected retinas and 32 LNA-anti–miR-23/27 injected retinas.

miR-23~27~24 Cluster Members in Angiogenesis. Our results are consistent with a recent report that silencing of miR-27b represses EC sprouting in vitro (16). Our results extend those findings to demonstrate that miR-23 and miR-27 are required for proper angiogenesis in vitro and in vivo. The following observations support our conclusion: (*i*) miR-23 and miR-27 are enriched in ECs and highly vascularized tissues; (*ii*) silencing of miR-23 or miR-27 in ECs impairs vascular network formation on Matrigel; (*iii*) knockdown of miR-23 or miR-27 in cultured aortic rings represses EC outgrowth, whereas adenoviral overexpression of miR-23 or miR-27 enhances aortic ring EC sprouting; (*iv*) knockdown of miR-23 or miR-27 represses EC proliferation and migration in response to VEGF; (*v*) silencing of miR-23 and miR-27 suppresses the sprouting of retinal vasculature in mice; and (*vi*) silencing of miR-23 and miR-27 represses neovascularization of the choroid in response to laser injury. It seems that miR-27 has a more dominant role in angiogenesis than miR-23, as shown by more severe miR-27 knockdown/overexpression phenotypes in the Matrigel and aortic ring assays. miR-24 has been shown to regulate apoptosis and inhibit cell proliferation (34, 35). In the absence of miR-23 and miR-27, there is a compensatory up-regulation of miR-24 in our in vitro and in vivo knockdown assays (Fig. 4*B*). The potential role of miR-24 in angiogenesis awaits future studies.

Regulation of Angiogenic Signaling by miR-23 and miR-27. The influence of miR-23 and miR-27 on angiogenesis can be attributed to their promotion of EC proliferation and migration in response to angiogenic factors. Consistent with this conclusion, knockdown of miR-23 and miR-27 represses MAPK signaling in response to VEGF, as shown by the repression of ERK1/2 phosphorylation. Phosphorylation of AKT is also repressed by miR-23 and miR-27 knockdown, which may result from the repression of VEGFR2 signaling by SEMA6A. Members of miRNA clusters have been proposed to function in combination (36). Axon guidance and MAPK signaling are highly ranked as the biological processes regulated by both miR-23 and miR-27. It is noteworthy, in this regard, that axon guidance molecules commonly affect EC behavior similarly, accounting for the similar patterning of both blood vessels and nerves (37), and MAPK pathways have been shown to regulate angiogenesis. Among the predicted target genes in these pathways, Sprouty proteins function as intracellular inhibitors of the MAPK pathway. Sema6A has also been reported to repress angiogenic signaling (27). We show that both miR-23 and miR-27 directly target the SPROUTY2 and SEMA6A 3′UTRs for repression. The identification of Sprouty2 as a target for both miR-23 and miR-27 is consistent with a recent report that Sprouty2 is a target for miR-27a during cancer cell growth and migration (38). The inhibitory actions of Sprouty proteins are mediated by interference of phosphorylation and activation of Raf, an upstream activator of the MAPK pathway. Repression of Sprouty2 by miR-23 and miR-27 at least partially underlies the mechanism whereby miR-23 and miR-27 enhance MAPK pathway activation in response to VEGF. sema6A may also contribute to the regulation of MAPK and PI3K-AKT signaling by miR-23 and miR-27, likely through repressing VEGFR2 signaling. Knockdown of Sprouty2 rescued the sprouting defects imposed by miR-23/27 silencing in cultured aortic rings, indicating a major role for Sprouty2 in mediating miR-23/27 angiogenic function. Because miR-23 and miR-27 have hundreds of predicted target genes, the angiogenic function of these miRNAs likely reflects the combined effects of multiple target genes.

miR-23~27~24 Cluster Members in CNV. Inflammation and angiogenesis play pivotal roles in CNV, the major cause of vision loss in patients with AMD (39, 40). Our results show that miR-23~27~24 cluster members are up-regulated in CNV (Fig. 6*A*). This correlates with the up-regulation of miR-23~27~24 cluster members by

proinflammatory stimuli (Fig. S5A) (41, 42), suggesting a role for miR-23~27~24 cluster members in linking inflammation to angiogenesis in CNV. Indeed, miR-27b was recently shown to contribute to LPS-mediated inflammation by targeting PPAR-γ (41). Our finding that silencing of miR-23 and miR-27 represses laser-induced CNV indicates that miR-23~27~24 cluster members indeed play a causative role in CNV. However, how miR-23, -27, and -24 regulate inflammation in CNV is yet to be investigated. Because miR-23~27~24 clusters are highly conserved from mice to humans, therapeutic manipulation of miR-23/27 represents a potential strategy in treating CNV in patients with neovascular AMD and other vascular diseases. The identification of miR-23 and miR-27 as important regulators of MAPK activation also suggests roles for these miRNAs in cancer.

Materials and Methods

LNA-Anti-miRs, Pre-miR Precursors, siRNAs, and miRNA expressing adenoviruses. LNA-anti-miRs for miR-23a/b, miR-27a/b, or scramble controls for in vitro and in vivo studies were synthesized from Exiqon. SiRNAs for SPROUTY2 were synthesized from Dharmacon. Sequences for SPROUTY2 siRNA, in vitro and in vivo LNA-anti-miRs, are described in *SI Materials and Methods*. Ambion pre-miR miRNA precursor of hsa-miR-23b, hsa-miR-27b, or negative control was synthesized from Applied Biosystem. Adenovirus expressing miR-23b, miR-27b, or lacZ was generated from mouse genomic DNA encoding miR-23b or miR-27 as described (24).

Cell Culture, Cell Proliferation, Scratch-Wound, In Vitro Matrigel, and Aortic Ring Sprouting Assay. HUVEC cell culture, cell proliferation, scratch-wound, in

vitro Matrigel assays, as well as aortic ring sprouting assays are described in *SI Materials and Methods*.

RNA, Western Blot Analysis, and Reporter Assay. RNA isolation, real-time RT-PCR, Western blot analysis, and reporter assays were performed according to standard procedures. Detailed methods are outlined in *SI Materials and Methods*.

Neonatal Retinal Injection, Postnatal Retinal Angiogenesis, and Laser-Induced CNV. In vivo injection in the mouse retina was performed primarily as described (43). Laser photocoagulation was induced in 6- to 8-wk-old male C57BL/6J mice as described (32). Detailed protocols are summarized in *SI Materials and Methods*.

Institutional Compliance and Animal Care. All experiments using animals were approved by the Institutional Animal Care and Use Committee at University of Texas Southwestern Medical Center.

1. Distler JH, et al. (2003) Angiogenic and angiostatic factors in the molecular control of angiogenesis. *Q J Nucl Med* 47:149–161.
2. Friedman E (2004) Update of the vascular model of AMD. *Br J Ophthalmol* 88:161–163.
3. Jager RD, Mieler WF, Miller JW (2008) Age-related macular degeneration. *N Engl J Med* 358:2606–2617.
4. Grisanti S, Tatar O (2008) The role of vascular endothelial growth factor and other endogenous interplayers in age-related macular degeneration. *Prog Retin Eye Res* 27:372–390.
5. Brown DM, et al.; ANCHOR Study Group (2006) Ranibizumab versus verteporfin for neovascular age-related macular degeneration. *N Engl J Med* 355:1432–1444.
6. Rosenfeld PJ, et al.; MARINA Study Group (2006) Ranibizumab for neovascular age-related macular degeneration. *N Engl J Med* 355:1419–1431.
7. Amrite A, Pugazhenthi V, Cheruvu N, Kompella U (2010) Delivery of celecoxib for treating diseases of the eye: influence of pigment and diabetes. *Expert Opin Drug Deliv* 7:631–645.
8. Zachary I (2005) Neuroprotective role of vascular endothelial growth factor: signalling mechanisms, biological function, and therapeutic potential. *Neurosignals* 14:207–221.
9. Small EM, Olson EN (2011) Pervasive roles of microRNAs in cardiovascular biology. *Nature* 469:336–342.
10. Bartel DP (2004) MicroRNAs: genomics, biogenesis, mechanism, and function. *Cell* 116:281–297.
11. Wang S, Olson EN (2009) AngiomiRs—key regulators of angiogenesis. *Curr Opin Genet Dev* 19:205–211.
12. Urbich C, Kuehbacher A, Dimmeler S (2008) Role of microRNAs in vascular diseases, inflammation, and angiogenesis. *Cardiovasc Res* 79:581–588.
13. Shen J, et al. (2008) MicroRNAs regulate ocular neovascularization. *Mol Ther* 16:1208–1216.
14. Poliseno L, et al. (2006) MicroRNAs modulate the angiogenic properties of HUVECs. *Blood* 108:3068–3071.
15. Suárez Y, Fernández-Hernando C, Pober JS, Sessa WC (2007) Dicer dependent microRNAs regulate gene expression and functions in human endothelial cells. *Circ Res* 100:1164–1173.
16. Kuehbacher A, Urbich C, Zeiher AM, Dimmeler S (2007) Role of Dicer and Drosha for endothelial microRNA expression and angiogenesis. *Circ Res* 101:59–68.
17. Harris TA, Yamakuchi M, Ferlito M, Mendell JT, Lowenstein CJ (2008) MicroRNA-126 regulates endothelial expression of vascular cell adhesion molecule 1. *Proc Natl Acad Sci USA* 105:1516–1521.
18. Chhabra R, Dubey R, Saini N (2010) Cooperative and individualistic functions of the microRNAs in the miR-23a~27a~24-2 cluster and its implication in human diseases. *Mol Cancer* 9:232.
19. Friedman RC, Farh KK, Burge CB, Bartel DP (2009) Most mammalian mRNAs are conserved targets of microRNAs. *Genome Res* 19:92–105.
20. Maragkakis M, et al. (2009) DIANA-microT web server: Elucidating microRNA functions through target prediction. *Nucleic Acids Res* 37(Web Server issue):W273–276.
21. Axton R, Wallis JA, Taylor H, Hanks M, Forrester LM (2008) Aminopeptidase O contains a functional nucleolar localization signal and is implicated in vascular biology. *J Cell Biochem* 103:1171–1182.
22. Wang S, et al. (2008) The endothelial-specific microRNA miR-126 governs vascular integrity and angiogenesis. *Dev Cell* 15:261–271.
23. Lee KS, et al. (2006) Troglitazone inhibits endothelial cell proliferation through suppression of casein kinase 2 activity. *Biochem Biophys Res Commun* 346:83–88.
24. Wang S, et al. (2008) Control of endothelial cell proliferation and migration by VEGF signaling to histone deacetylase 7. *Proc Natl Acad Sci USA* 105:7738–7743.
25. Papadopoulos GL, Alexiou P, Maragkakis M, Reczko M, Hatzigeorgiou AG (2009) DIANA-mirPath: Integrating human and mouse microRNAs in pathways. *Bioinformatics* 25:1991–1993.
26. Impagnatiello MA, et al. (2001) Mammalian sprouty-1 and -2 are membrane-anchored phosphoprotein inhibitors of growth factor signaling in endothelial cells. *J Cell Biol* 152:1087–1098.
27. Dhanabal M, et al. (2005) Recombinant semaphorin 6A-1 ectodomain inhibits in vivo growth factor and tumor cell line-induced angiogenesis. *Cancer Biol Ther* 4:659–668.
28. Casci T, Vinós J, Freeman M (1999) Sprouty, an intracellular inhibitor of Ras signaling. *Cell* 96:655–665.
29. Toyofuku T, et al. (2004) Dual roles of Sema6D in cardiac morphogenesis through region-specific association of its receptor, Plexin-A1, with off-track and vascular endothelial growth factor receptor type 2. *Genes Dev* 18:435–447.
30. Stahl A, et al. (2010) The mouse retina as an angiogenesis model. *Invest Ophthalmol Vis Sci* 51:2813–2826.
31. Ryan SJ (1982) Subretinal neovascularization. Natural history of an experimental model. *Arch Ophthalmol* 100:1804–1809.
32. Tobe T, et al. (1998) Targeted disruption of the FGF2 gene does not prevent choroidal neovascularization in a murine model. *Am J Pathol* 153:1641–1646.
33. Campa C, et al. (2008) Effects of an anti-VEGF-A monoclonal antibody on laser-induced choroidal neovascularization in mice: optimizing methods to quantify vascular changes. *Invest Ophthalmol Vis Sci* 49:1178–1183.
34. Lal A, et al. (2009) miR-24 Inhibits cell proliferation by targeting E2F2, MYC, and other cell-cycle genes via binding to "seedless" 3'UTR microRNA recognition elements. *Mol Cell* 35:610–625.
35. Walker JC, Harland RM (2009) microRNA-24a is required to repress apoptosis in the developing neural retina. *Genes Dev* 23:1046–1051.
36. Yuan X, et al. (2009) Clustered microRNAs' coordination in regulating protein-protein interaction network. *BMC Syst Biol* 3:65.
37. Carmeliet P, Tessier-Lavigne M (2005) Common mechanisms of nerve and blood vessel wiring. *Nature* 436:193–200.
38. Ma Y, Yu S, Zhao W, Lu Z, Chen J (2010) miR-27a regulates the growth, colony formation and migration of pancreatic cancer cells by targeting Sprouty2. *Cancer Lett* 298:150–158.
39. Bressler SB (2009) Introduction: Understanding the role of angiogenesis and antiangiogenic agents in age-related macular degeneration. *Ophthalmology* 116(Suppl 10):S1–S7.
40. Augustin AJ, Kirchhof J (2009) Inflammation and the pathogenesis of age-related macular degeneration. *Expert Opin Ther Targets* 13:641–651.
41. Jennewein C, von Knethen A, Schmid T, Brüne B (2010) MicroRNA-27b contributes to lipopolysaccharide-mediated peroxisome proliferator-activated receptor gamma (PPARgamma) mRNA destabilization. *J Biol Chem* 285:11846–11853.
42. Zhou R, et al. (2009) NF-kappaB p65-dependent transactivation of miRNA genes following Cryptosporidium parvum infection stimulates epithelial cell immune responses. *PLoS Pathog* 5:e1000681.
43. Matsuda T, Cepko CL (2004) Electroporation and RNA interference in the rodent retina in vivo and in vitro. *Proc Natl Acad Sci USA* 101:16–22.